

# Advanced spinel and sub- $\mu\text{m}$ $\text{Al}_2\text{O}_3$ for transparent armour applications

Andreas Krell\*, Jens Klimke, Thomas Hutzler

*Fraunhofer Institute for Ceramic Technologies and Systems, Dresden, Germany*

Available online 12 May 2008

## Abstract

Hardness is important for a high ballistic strength, and with  $\text{HV}_{10} = 20\text{--}22$  GPa sintered sub- $\mu\text{m}$   $\text{Al}_2\text{O}_3$  is the hardest of all transparent materials for compact windows. However, light transmission through polycrystalline  $\text{Al}_2\text{O}_3$  is limited by birefringent scattering losses: high transmissions are known at larger IR wavelengths for grain sizes of about  $0.5\ \mu\text{m}$  but the visible real in-line transmission RIT is only 70–75% of the theoretical maximum at 0.8–1 mm thickness. These losses will be the higher for thicker components whereas a safe ballistic performance requires 1.5–2 mm thickness at least. New technologies bring the transmission closer to the limit associating grain sizes of  $0.3\ \mu\text{m}$  with an RIT of 84–93% of the theoretical maximum (thickness 0.8 mm). However, even these extreme results give again rise to doubt that it will ever be possible to manufacture larger and thicker  $\text{Al}_2\text{O}_3$  windows with a sufficiently high transparency.

On the other hand, new results are presented for fine-grained spinel with RIT close to the theoretical maximum and with a hardness that approaches sapphire. In first ballistic tests this spinel outperformed sapphire of different orientations. It is, therefore, suggested that sub- $\mu\text{m}$   $\text{Al}_2\text{O}_3$  may be a good choice for IR windows or as armour for low threat applications where thinner tiles can be used. Most threats, however, require thicker windows where the new spinel appears as one of the most favourable candidates.

© 2008 Elsevier Ltd. All rights reserved.

**Keywords:** Transparent armour; Light transmission; Defect-free processing; Alumina  $\text{Al}_2\text{O}_3$ ; Spinel  $\text{MgO}\cdot\text{Al}_2\text{O}_3$

## 1. Introduction

Small grain sizes limit the space for motion and multiplication of the lattice elements of microplasticity (dislocations, twins). Thus, decreasing grain sizes give rise to a higher hardness as far as grain boundary instability does not deteriorate the hardness in extremely fine (nanoscale) microstructures. As a result, sub- $\mu\text{m}$  sintered  $\text{Al}_2\text{O}_3$  exhibits a Vickers macro-hardness  $\text{HV}_{10} > 20$  GPa (at testing load of 10 kgf).<sup>1</sup> These ceramics become transparent when manufactured with high purity  $>99.9\%$  and when the residual porosity is reduced completely. Hence, sub- $\mu\text{m}$   $\text{Al}_2\text{O}_3$  is the hardest and strongest of all transparent armour materials that can be used for compact windows.<sup>2</sup> Hardness is most important for this use since the ballistic strength (the shielding effect of a ceramic tile in front of some backing) increases with the hardness (Fig. 1).<sup>3</sup>

On the other hand, however, light transmission through polycrystalline  $\text{Al}_2\text{O}_3$  is subject not only to absorption and to scattering by pores (as in all other transparent materials) but

is additionally decreased by losses caused by the birefringent splitting of the beam on each crossover from one crystal to the next (Fig. 2A). The one way to minimise birefringent scattering losses is a small sub- $\mu\text{m}$  grain size such that the electromagnetic wave package does not “see” individual crystals. Typically, with a grain size of highly dense sintered  $\text{Al}_2\text{O}_3$  of about  $0.5\ \mu\text{m}$  the “real” in-line transmission  $\text{RIT}^a$  is about 60% ( $\sim 70\%$  of theoretical limit<sup>b</sup>) at 1 mm thickness and with a wavelength of  $\lambda = 640$  nm.

All these losses (e.g. 30% over 1 mm of thick dense sub- $\mu\text{m}$   $\text{Al}_2\text{O}_3$ ) increase with the thickness. Thus, in sintered  $\text{Al}_2\text{O}_3$  the additional birefringent scattering leads to a much stronger thickness effect than known from isotropic transparent materials (Fig. 2B).

Spinel ( $\text{MgO}\cdot\text{Al}_2\text{O}_3$ ) is one of these cubic oxides where because of the absence of birefringent scattering high transmis-

<sup>a</sup> Only the unscattered “in-line” light contributes to clear images. Therefore, a valid characterisation of transparency has to exclude scattered amounts and a “real” in-line transmission was defined that is measured with a small aperture (half of opening angle) of about  $0.5^\circ$ .<sup>2</sup>

<sup>b</sup> Maximum transmission  $T_{\text{th}} = 100\% - \text{reflection}$  (two surfaces).  $T_{\text{th}} = 2n/(n^2 + 1)$  is governed by  $n$  (refractive index).

\* Corresponding author.

E-mail address: [andreas.krell@ikts.fraunhofer.de](mailto:andreas.krell@ikts.fraunhofer.de) (A. Krell).

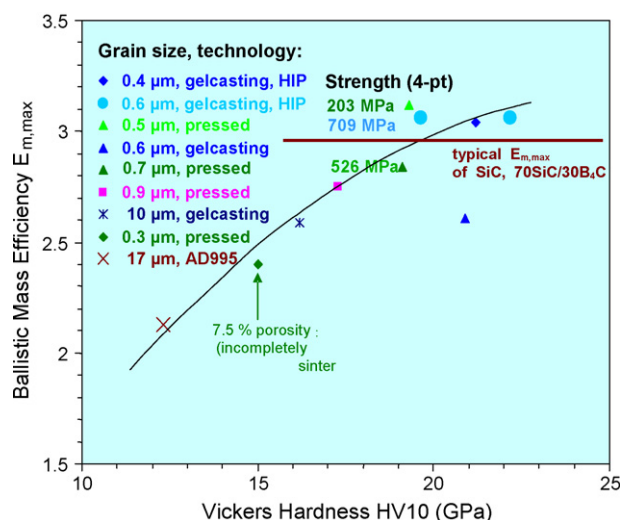


Fig. 1. Influence of hardness on the maximum mass efficiency of  $\text{Al}_2\text{O}_3$  (DoP [Depth of Penetration] tests with steel backing, tungsten rod penetrator with mass 44 g, aspect ratio 3.2, impact velocity 1250 m/s).

sion values can generally be obtained with larger grain sizes, i.e. higher temperatures can be applied to remove the last pores (as far as exaggerated growth does not result in intragranular porosity). Higher transmission reduces the detrimental thickness effect, and it is a general experience that really transparent windows are obtained much more easily with such cubic ceramics than with  $\text{Al}_2\text{O}_3$ . As an example, Fig. 3 compares the different degrees of transparency of typical advanced alumina and spinel ceramics.

Starting with the extended experience of mechanical advantages of *fine*-grained ceramics, first efforts to develop transparent spinel armour were directed towards small grain sizes,<sup>4</sup> but the associated low sintering temperature did not provide the requested high degree of transparency. In the following decades the residual porosity was, therefore, eliminated by higher temperatures while accepting more grain growth. Unfortunately, the mechanical parameters of known cubic transparent ceramics are generally inferior to (non-cubic) corundum, and the focus on apparently tolerable grain growth with sizes of 50–300  $\mu\text{m}$ <sup>5–7</sup> was accompanied by a further reduction of the mechanical parameters (as an example, the hardness of such coarse transparent spinel is only about  $\text{HV}_{10} = 12 \text{ GPa}$ ).<sup>8</sup>

The target of the present investigations was, therefore, a twofold:

- Check of technological approaches which could be able to increase the transparency of sintered  $\text{Al}_2\text{O}_3$  in way that the real in-line transmission comes close to the theoretical maximum (in turn to minimise the detrimental thickness effect). Probably, with birefringent  $\text{Al}_2\text{O}_3$  this means the development of new microstructures which associate an extreme purity with smallest grain sizes  $<0.5 \mu\text{m}$  at zero porosity.
- On the other hand, it was another objective to develop highly transparent spinel ceramics with a ballistic resistance close to that of sub- $\mu\text{m}$  alumina. The investigation had to check out whether this can be achieved by associating a high trans-

parency with a higher hardness enabled by new fine-grained spinel microstructures.

## 2. Improving light transmission through sintered $\text{Al}_2\text{O}_3$

### 2.1. Processing of new transparent corundum ceramics

The need to eliminate *last hundredths* of a percent of porosity holds for any *transparent* material, be it of glassy, single or polycrystalline nature. The technological challenge is, however, much tougher when it has to be achieved with pure solid state sintering<sup>c</sup> and associated with a minimum of grain growth, i.e. at low temperatures.

With all these difficulties it is obvious that transparency needs very special, optimized sintering regimes. The most common approach today is pressureless pre-sintering up to closed porosity followed by hot-isostatic post-densification (HIP—hot-isostatic pressing).<sup>2</sup> Other approaches like microwave and millimetre wave sintering<sup>9–11</sup> or spark plasma sintering (SPS)<sup>12</sup> may provide similar results (until present, however, without improvements of dense microstructures and their properties)<sup>13,11</sup> but are often limited to bodies with simple shape (e.g. discs).

On the other hand it has to be emphasised that the development and application of an optimized sintering approach is imperative but is *not the key* to high transparency: even the most advanced HIP regime will not provide transparent components without (i) selection of the *right raw powder* together with (ii) application of a very special, *defect avoiding processing*.<sup>14</sup> Since nanoscale powders with particles  $<100 \text{ nm}$  tend to agglomerate, the condition of best homogeneity of particle coordination is achieved more successfully with particle sizes between 100 and 200 nm, and recent porosity investigations of green shaped bodies have revealed a close correlation of the *best homogeneity* (obtained by liquid shaping of high solid loading slurries with ideal state of dispersion) with *lowest sintering temperatures* and *smallest grain sizes* (at density  $>99.97\%$ ).<sup>15</sup> As a result, a fairly high degree of transparency was observed previously by gelcasting of 150 nm corundum powder with purity  $>99.99\%$   $\text{Al}_2\text{O}_3$  (Fig. 3a).<sup>2</sup>

It was shown recently (Fig. 4a) that the homogeneity of particle coordination can be improved further when using the same powder gelcasting (with 4–5 wt% of a monomer binder) is substituted by binder-free slip-casting into porous  $\text{Al}_2\text{O}_3$  moulds (porosity  $\sim 40\%$ , average pore size 54 nm, purity 99.9%); the one organic additive in this slurry was a dispersant<sup>d</sup> (0.8 wt% related to  $\text{Al}_2\text{O}_3$ ).<sup>15</sup> Annealing was performed in air where burn-out of organic additives was completed on heating to 800 °C without isothermal hold. Then the samples were heated to higher temperatures with a rate of 2 K/min to closed porosity (relative density  $\sim 96\%$ ) with final densi-

<sup>c</sup> Because of optical homogeneity transparent ceramics have to be single phase materials that cannot be sintered with an additive of several percents of a *liquid* phase.

<sup>d</sup> Dolapix CE64, Zschimmer & Schwarz, Lahnstein, Germany.

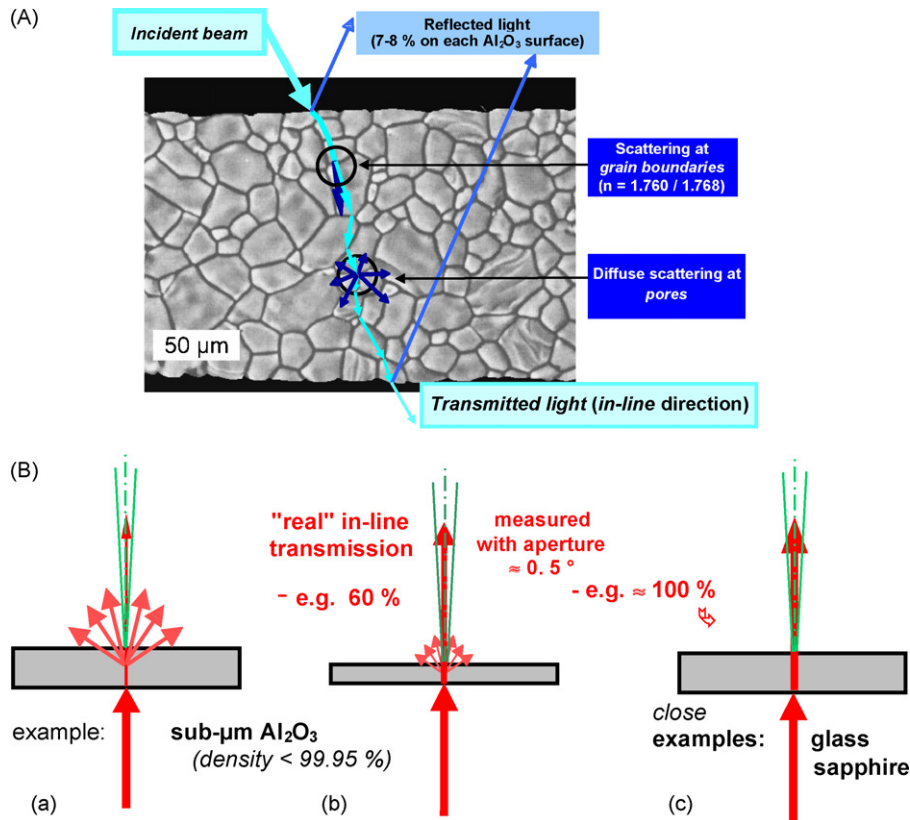


Fig. 2. (A) Light transmission through polycrystalline translucent (coarse grained)  $\text{Al}_2\text{O}_3$ . Without absorption, intensity losses are caused by (i) reflection on both surfaces (about 14% with refractive index  $n = 1.765$ ), (ii) diffuse scattering at pores and (iii) birefringent scattering (not active in *cubic* [= optically isotropic] crystallites). (B) Scattering or absorption losses ( $\rightarrow$  in-line transmission < 100%) give rise to a significant thickness effect (b  $\rightarrow$  a). It disappears when the transmission approaches the theoretical maximum (c).

fication by hot-isostatic pressing in argon at a pressure of 200 MPa.

## 2.2. Results: comparing slip-casting with gelcasting

Fig. 5 compares the most fine-grained microstructures obtained by gelcasting and by slip-casting and gives the optimum HIP conditions and the resulting real in-line transmissions RIT of optimized batches (for thickness 0.8 mm at  $\lambda = 640$  nm). The lower sintering temperature after slip-casting (Fig. 4b) reduces the grain size by an extent which may appear small as any absolute difference of small values is small, but on a relative scale the slip-cast grain size is just 62% of the optimum observed after gelcasting.

As a consequence, the transparency was increased to high RIT values which before these investigations were regarded physically hardly probable (note that  $\text{RIT} = 72\text{--}80\%$  are absolute values which equal 0.84–0.93 of the theoretical maximum of birefringent alumina).

## 3. Development of fine-grained transparent spinel ceramics

### 3.1. Manufacture and resulting properties

A central problem with most transparent cubic ceramics is the difficult situation of raw powders: whereas high-purity alu-

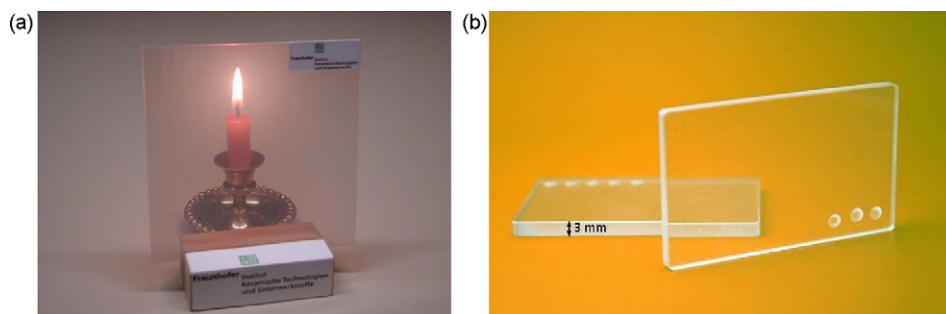


Fig. 3. Transparent sintered armour ceramics. (a) 0.8-mm thin sub- $\mu\text{m}$  alumina and (b) 3-mm thick spinel.

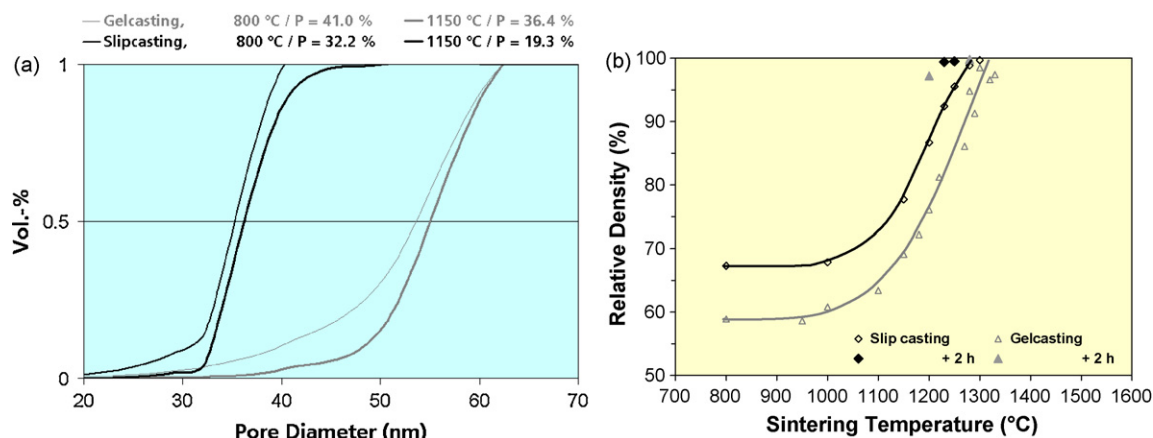


Fig. 4. (a) Closer and more narrow pore size distribution in slip-cast green bodies of a 150 nm corundum powder compared with gelcasting and (b) resulting densification on sintering (void symbols: densities obtained after heating to indicated temperature without isothermal hold; full symbols give additional results with 2 h of annealing)<sup>15</sup>.

mina powders are available with most different particle sizes, most commercial spinel powders are either insufficiently pure or exhibit very coarse or extremely fine particles (e.g. with sizes of about 50 nm which oppose the defect-avoiding liquid shaping approaches because of low possible solid loadings).

In this difficult situation, the present investigation has compared three basically different approaches:

- (i) Fine-grained transparent spinel by *processing of commercial spinel powders*. Only this approach was used to manufacture first 100 mm × 100 mm tiles for ballistic investigation.
- (ii) Development of transparent spinel from a *new chemical synthesis* of spinel powder.
- (iii) Transparent spinel by *reactive sintering* of a “granulometric optimum” and high-purity Al<sub>2</sub>O<sub>3</sub> powder mixed with MgO.

### 3.1.1. Processing of commercial spinel powders

Two different 99.99% pure spinel powders were selected, one with a specific surface of 28 m<sup>2</sup>/g (particle size 50–100 nm) and another one with 15 m<sup>2</sup>/g. Both grades were dispersed in water,

and different means had to be applied (ultrasonification, milling) for complete desintegration of agglomerates before plate-like bodies could be shaped. The performance of the 15 m<sup>2</sup>/g powder was more difficult because the size of primary particles was similar as in the powder with the higher specific surface with, however, a much higher degree of aggregation (probably as a consequence of a higher temperature of calcination at the manufacturer).

Sintering additives like LiF as known from other investigations<sup>5–7</sup> were not used here because it turned out less favourable for the development of highly dense and fine-grained microstructures. The pre-sintering and HIP conditions were the same as described above for Al<sub>2</sub>O<sub>3</sub>.

Similarly fine-grained, highly transparent and hard tiles could be obtained with both powders (Fig. 6) in spite of their different technological performance. By slight variations of the desintegration approach, with use of small doping additives (<0.5%) and with manipulation of the sintering temperatures it was possible to tune the average grain size between about 0.4 and 5 μm without loss of transparency. The lowest hardness was HV10 = 13 GPa observed for a microstructure with 5.5 μm average grain size after HIP at 1650 °C.

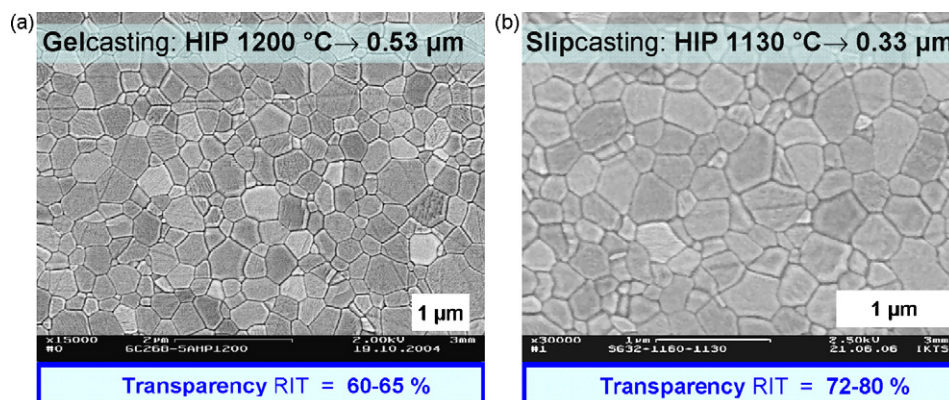


Fig. 5. HIP temperatures, average grain sizes and RIT transmission values after optimized (a) gelcasting and (b) slip-casting of a 150 nm corundum powder. The given RIT ranges refer to averages of different batches.



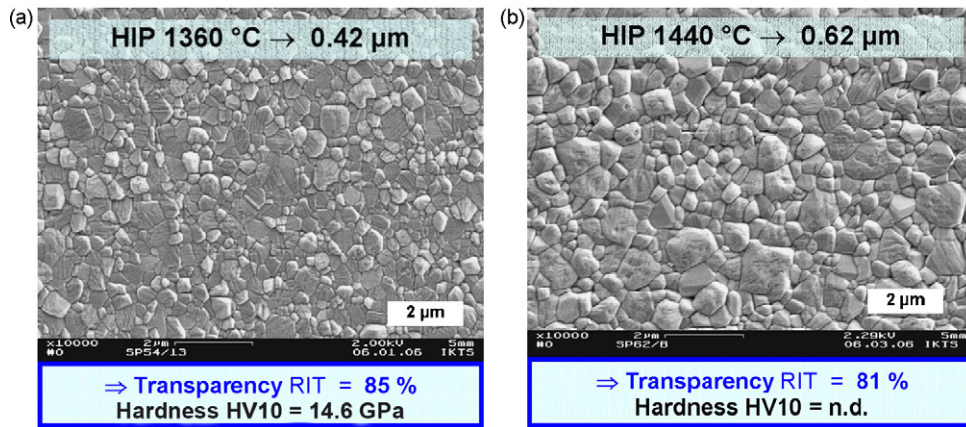


Fig. 6. HIP temperatures, average grain sizes, RIT transmission values and macrohardness HV10 of sintered transparent spinel manufactured starting from different commercial powders: (a) specific surface  $28 \text{ m}^2/\text{g}$  (European manufacturer), (b)  $15 \text{ m}^2/\text{g}$  (American manufacturer). RIT data for thickness 0.8 mm and  $\lambda = 640 \text{ nm}$ .

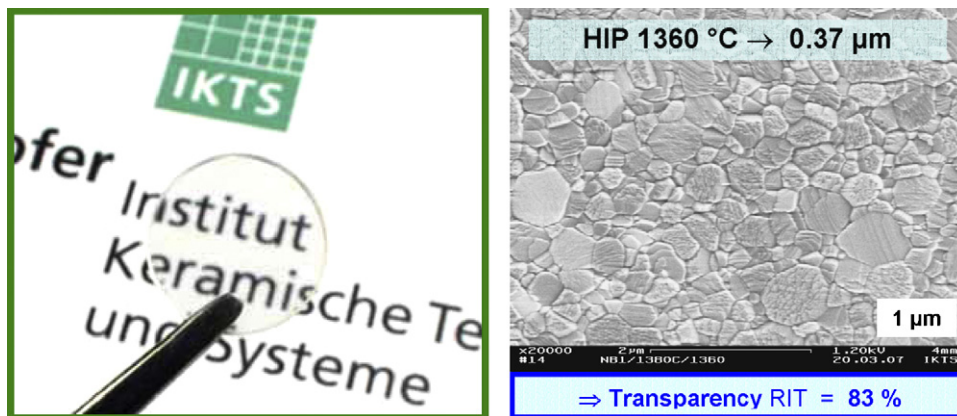


Fig. 7. Spinel from powder of new chemical synthesis. HIP temperature, average grain size and RIT transmission (referred to 0.8 mm thickness,  $\lambda = 640 \text{ nm}$ ; absolute RIT of the 1.6-mm thick disc: 80%).

### 3.1.2. Chemical synthesis of new spinel powder

Aqueous processing started from inorganic salts as described by a proprietary corundum syntheses,<sup>16</sup> here with additive of a magnesia precursor. After calcination at  $900^\circ\text{C}$ , the specific surface was  $49 \text{ m}^2/\text{g}$ .

Powder processing and sintering was the same as outlined above for the commercial spinel powders. The sintering temperature was similar as observed for the commercial powder with a specific surface of  $28 \text{ m}^2/\text{g}$ . The grain size, however, was once more reduced (Fig. 7).

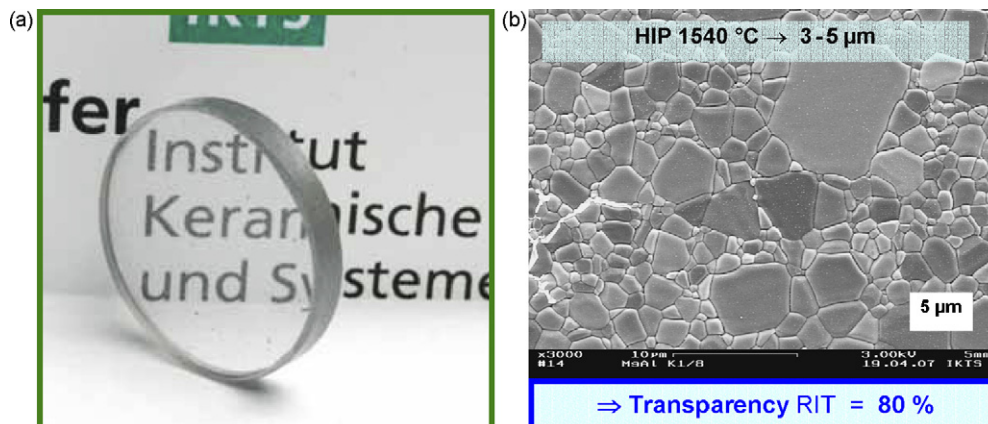


Fig. 8. HIP temperature, average grain size and RIT transmission (for thickness 0.8 mm,  $\lambda = 640 \text{ nm}$ ) of a disc manufactured by reactive sintering of mixed  $\text{Al}_2\text{O}_3$  and  $\text{MgO}$  powders (no dopant).

Table 1  
Basic mechanical data of sapphire, sintered transparent sub- $\mu\text{m}$   $\text{Al}_2\text{O}_3$  and Mg–Al spinel

	Sapphire	Sintered $\text{Al}_2\text{O}_3$	Sintered Mg–Al spinel
Young's modulus (GPa)	~400	~400	~275
Hardness HV10 (GPa)	15–16	20.5–21.5	14.5–15.0
4-point bending strength (MPa)	400–600	600–700	200–250
Compressive strength (MPa)	~2000	Not determined	Not determined
$K_{\text{IC}}$ (MPa/ $\sqrt{\text{m}}$ )	2.0–2.8	~3.5	~1.8–2.2

### 3.1.3. Reactive sintering of $\text{Al}_2\text{O}_3 + \text{MgO}$

The process started with preparation of an aqueous dispersion of the same high-purity corundum powder as used above for the manufacture of transparent sub- $\mu\text{m}$  sintered  $\text{Al}_2\text{O}_3$  (particle size about 150 nm, specific surface 13–14 m<sup>2</sup>/g). This powder was mixed with a coarse magnesia powder (particle size 2–3  $\mu\text{m}$ , specific surface 5–7 m<sup>2</sup>/g). After co-milling, the MgO particle size was still about three times that of the corundum powder. Compaction and sintering were performed as for samples of commercial spinel powders (no doping additive).

Surprisingly, this big difference of the particle sizes did not hinder homogeneous reaction (spinel formation was completed at about 1150–1200 °C) and sintering densification. Fig. 8 shows the result.

### 3.2. Results of ballistic evaluation

Ceramic tiles were manufactured with a lateral dimension of about 100 mm  $\times$  100 mm and with different thicknesses by the following processes:

- (i) sub- $\mu\text{m}$   $\text{Al}_2\text{O}_3$  by gelcasting (Figs. 3–5a),

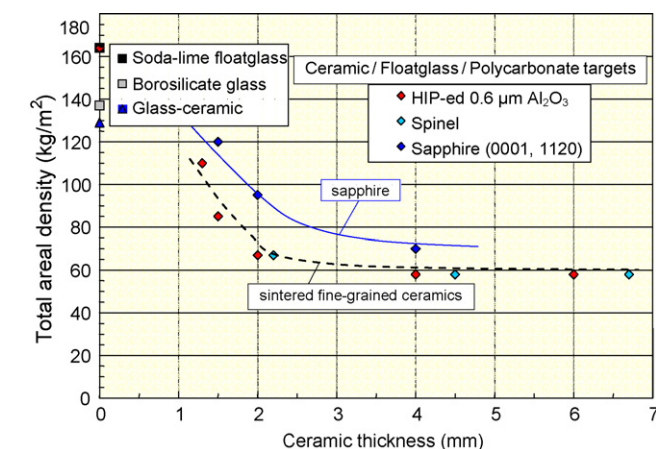


Fig. 9. Results of perforation tests ( $v_{\text{projectile}} = 850$  m/s, AP ammunition).<sup>17</sup> The data on the y-axis give the areal densities of two glasses and a glass-ceramic which stop the projectile (associated thickness  $\approx 60$  mm), the curves show how the total areal density of composite targets with soda-lime floatglass/polycarbonate backing is reduced by thin ceramic fronts: 1.5-mm thin front plies of sub- $\mu\text{m}$  sintered  $\text{Al}_2\text{O}_3$  reduce the normalized areal density which stops the projectile by 50% (note, however:  $\text{Al}_2\text{O}_3$  is not fully transparent at thickness  $> 1$  mm!), and a similar stability is obtained with fine-grained sintered spinel that outperforms sapphire and exhibits a real in-line transmission close to the theoretical limit.

- (ii) transparent spinel with average grain size 1.7  $\mu\text{m}$  by the approach of Section 3.1.1 (similar ballistic results were observed for batches with average grain sizes of 0.5 and 5.5  $\mu\text{m}$ ).

Perforation tests of ceramic/glass (15–30 mm)/polycarbonate (4 mm) targets with 7.62 mm  $\times$  51 AP ammunition ( $v_{\text{projectile}} = 850$  m/s) compared the ballistic performance of these two ceramics with sapphire fronts of two different orientations ((0001), (1120))<sup>17</sup>; Table 1 gives basic mechanical data of the target materials.

Compared with sapphire (similar performance of both orientations, eventually with slightly better performance of (1120)), the advantage of sintered  $\text{Al}_2\text{O}_3$  in the ballistic results of Fig. 9 is explained by the higher hardness of the ceramic (HV10–21 GPa compared to 15–16 GPa for sapphire with these orientations). Most surprising, however, is the performance of the transparent fine-grained spinel which comes close to the ballistic strength of sub- $\mu\text{m}$   $\text{Al}_2\text{O}_3$  and outperforms sapphire in these tests—despite lower spinel values of all basic data (Table 1).

An explanation of the discrepancy between the high ballistic strength of the fine-grained spinel (Fig. 9) and its relatively low basic properties (Table 1) is beyond the frame of the present comparative investigation. A first more fundamental approach of understanding was presented to public discussion on a recent conference.<sup>17</sup>

## 4. Conclusions

Sub- $\mu\text{m}$  sintered corundum ( $\text{Al}_2\text{O}_3$ ) is the hardest of all transparent armour ceramics, and in the visible range its real in-line transmission RIT can be increased to  $\sim 90\%$  of theoretical limit (at 1 mm thickness) by means of extreme homogenous slip-casting. However, there is doubt whether slip-casting will ever provide larger components as requested for most armour applications, and even the present extreme progress of an RIT with only 10% of losses over a thin thickness of 1 mm means less transparency at a thickness of, e.g. 2 or 3 mm. Therefore, even these advanced microstructures will not be “fully transparent” at a typical thickness of a ceramic front ply.

On the other hand, however, it was demonstrated that fine-grained and almost “fully transparent” spinel armour can be provided with grain sizes in the micrometre or, as well, in the sub- $\mu\text{m}$  range with a resulting high hardness HV10 = 14.5–15 GPa and with a ballistic strength which comes close to sub- $\mu\text{m}$   $\text{Al}_2\text{O}_3$  and which is able to outperform sapphire. These new spinel

grades appear, therefore, as favourable candidates for the protection against threats which require thicker ceramic windows.

## Acknowledgements

The present work uses results from investigations at IKTS Dresden and at EMI Freiburg performed with financial support of the German Ministry of Defence under contracts E/E210/0D008/I1452, E/E91S/3A621/T5185, and E/E91S/4A299/3F034. Other parts of this work were funded by an internal project “MMM Tools: Multiscale Materials Modeling” of the Fraunhofer Society. All ballistic investigations were performed by E. Strassburger at EMI Freiburg.

## References

1. Krell, A., Improved hardness and hierarchic influences on wear in submicron sintered alumina. *Mater. Sci. Eng. A*, 1996, **209**(1–2), 156–163.
2. Krell, A., Blank, P., Ma, H., Hutzler, T., Van Bruggen, M. and Apetz, R., Transparent sintered corundum with high hardness and strength. *J. Am. Ceram. Soc.*, 2003, **86**(1), 12–18.
3. Krell, A. and Strassburger, E., High-purity submicron  $\alpha$ - $\text{Al}_2\text{O}_3$  armor ceramics: design, manufacture, and ballistic performance. *Ceram. Trans.*, 2001, **134**(1–2), 463–471.
4. Gazza, G. E. and Dutta, S. K., Hot pressing of ceramic oxides to transparency by heating in isothermal increments, Patent US 3,767,745, Int. Class. IPK7 C04B35/64, 23.10.1973.
5. Gilde, G., Patel, P., Patterson, P., Blodgett, D., Duncan, D. and Hahn, D., Evaluation of hot pressing and hot isostatic pressing parameters on the optical properties of spinel. *J. Am. Ceram. Soc.*, 2005, **88**(10), 2747–2751.
6. Reimanis, I. E., Kleebe, H.-J., Cook, R. L. and DiGiovanni, A., Transparent spinel fabricated from novel powders: synthesis, microstructure and optical properties. In *SPIE Proceedings of Defense and Security Symposium, Orlando (FL)*, 13.–15.4.2004. The Society of Photo-optical Instrumentation Engineers, Bellingham, WA, 2004.
7. Cook, R., Kochis, M., Reimanis, I. and Kleebe, H.-J., A new powder production route for transparent spinel windows: powder synthesis and window properties. In *SPIE Proceedings of Vol. 5786 (Defence and Security Symposium 2005, IX. Window and Dome Technologies and Materials, Orlando [FL], 28.3.2005)*, ed. R. W. Tustison. The Society of Photo-Optical Instrumentation Engineers, Bellingham, WA, 2005, pp. 41–47.
8. Patel, P. J., Gilde, G. A., Dehmer, P. G. and McCauley, J. W., Transparent armor. *AMPTIAC Newsletter*, 2000, **4**(3), 1–13.
9. Cheng, J., Agrawal, D., Zhang, Y., Drawl, B. and Roy, R., Fabricating transparent ceramics by microwave sintering. *Bull. Am. Ceram. Soc.*, 2000, **79**(9), 71–74.
10. Cheng, J., Agrawal, D., Zhang, Y. and Roy, R., Microwave sintering of transparent alumina. *Mater. Lett.*, 2002, **56**(4), 587–592.
11. Link, G. and Thumm, M., Detailed investigations in microwave sintering of ceramics by means of dilatometer. In *Proceedings of the International Workshop on Strong Microwaves in Plasmas*, Vol. 2, ed. A. G. Litvak, 2002, pp. 719–724.
12. Dobedoe, R. S., West, G. D. and Lewis, M. H., Spark plasma sintering of ceramics. *Bull. Eur. Ceram. Soc.*, 2003, **1**(1), 19–24.
13. Krell, A. and van Bruggen, M. P. B., Comments on Spark plasma sintering of ceramics. *Bull. Eur. Ceram. Soc.*, 2004, **2**(1), 35.
14. Krell, A. and Ma, H.-W., Sintering transparent and other sub- $\mu\text{m}$  alumina. *The Right Powder, cfi/Ber. Dt. Keram. Ges.*, 2003, **80**(4), E41–E45.
15. Krell, A. and Klimke, J., Effect of the homogeneity of particle coordination on solid state sintering of transparent alumina. *J. Am. Ceram. Soc.*, 2006, **89**(6), 1985–1992.
16. Ma, H. and Krell, A., Method of producing aluminum oxides and products obtained on the basis thereof, Patent US 6,841,497 B1, Int. Class. IPK7 C08B35/10, 11.01.2005.
17. Krell, A. and Strassburger, E., Hierarchy of key influences on the ballistic strength of opaque and transparent armor. *Ceram. Eng. Sci. Proc.*, 2007, **28**(5) (“Advances in Ceramic Armor III”; Daytona Beach Conf., Jan 21–26 2007) 45–55, Am. Ceram. Soc. and Wiley & Sons, Hoboken, 2007).